The effect of localized ionospheric perturbations on subionospheric VLF propagation on the basis of finite element method

K. Baba[1] and M. Hayakawa[2]

[1] Department of Electronics Engineering, Chubu University, Kasugai Aichi 487, Japan
[2] The University of Electro-Communications, Chofu Tokyo 182, Japan

Abstract. The purpose of this paper is to propose the use of finite element method in investigating the effect of localized perturbations in the lower ionosphere on subionospheric VLF propagation. Due to the complexity of the method, we have analyzed only a two-dimensional case where a localized perturbation lies on the great circle path between the transmitter and receiver. The formulation is first made, and a few computational results are presented in order to indicate the effectiveness of this finite element method.

1. Introduction

Transient perturbations in the lower ionosphere are known to be produced by pitch-angle diffusion of whistler-electron resonance near the magnetospheric equatorial plane and subsequent electron precipitation into the lower ionosphere. These ionospheric perturbations can be detected by variations in the amplitude and phase of subionospheric VLF signals, and these signal variations are referred to as "Trimpi effects"(Helliwell, et al.,1973;a recent review by Rycroft,1991). An initially accepted model was based on the assumption that the perturbations lie on the great circle(GC) path from the transmitter to the receiver and extend to infinity in the horizontal direction perpendicular to the GC path (Tolstoy et al., 1986). Analysis of observed data has indicated a need for more realistic treatment which could estimate the effect of scattering by the ionization enhancement located off the GC path (Inan and Carpenter, 1987; Dowden and Adams, 1988). Poulsen et al.(1990) have developed a three-dimensional model of subionospheric VLF propagation in the presence of localized perturbations which is based on the approximate theory. However, for the steep gradients of density perturbations in the horizontal direction, multiple mode conversion cannot be neglected and additional higher order modes of comparable strength may be propagating in the region considered. Moreover, it is of great importance to estimate how mode 1 re-distributes its energy into subsquent modes 1,2 etc.

Since a considerable number of Trimpi events are such that the perturbations lie on the GC path (a two-dimensional case), this 2-D problem is still the current topic to be pursued with great interest. In an excellent paper by Tolstoy et al.(1986) dealing with the 2-D case, they estimated the changes of the fields produced by the perturbation by the 2-D mode theory by Pappert and Snyder (1972), which employs a multi-slab approximation to the horizontal inhomogeneities. However, their model neglects reflection at the slab boundaries and approximates the fields within each slab by the expansions of some finite number of modal functions. In this paper we propose the use of finite element method (FEM)(Baba and Hayakawa, 1993) for this 2-D case, and this FEM provides us with exact estimation of wave fields yielding the changes in amplitude and phase that would be produced by the perturbation. In other words, this FEM removes the above-mentioned two drawbacks involved in Tolstoy et al. (1986), and the method is applicable for any perturbations including steep gradients.

2. Finite Element Formulation

In this section we describe the formulations of finite element method for the analysis of VLF radio wave propagation in the Earth-ionosphere waveguide. Fig.1(a) shows a schematic 2-D model of the Earth-ionosphere waveguide propagation in the presence of localized perturbations to lie on the GC path between the transmitter and receiver. The details of this FEM application are published in Baba and Hayakawa (1993), and so we do not describe them again here.

3. Ionosphere Models

The collision frequency of electrons used for calculation is given as follows.

$$\nu(z) = 5 \times 10^6 \exp\{-0.15(z - 70)\} \qquad [s^{-1}] \qquad (1)$$

where z is a height above the ground in km. The region indicated as "inhomogeneous region" in Fig.1(b), includes two sources of inhomogeneity; (1)background profile and (2) the perturbation due to a Trimpi effect. The variation of density perturbations with distance in both horizontal and vertical directions

is represented by Gaussian distributions. Therefore, the perturbed electron density profiles used for calculation are given as follows,

$$N(z) = N_0(z) \cdot \{1 + EN \cdot \exp\{-(z - z_0)^2/sz^2 - (x - x_0)^2/sx^2\}$$
$$N_0(z) = 30.74 \exp\{0.24(z - 87)\} \qquad [cm^{-3}] \tag{2}$$

where $N_0(z)$ is the background nighttime density profile(Reagan et al.,1982), and is illustrated by a full line in Fig.2. EN is an enhancement factor, that is, the maximum difference between the perturbed electron density and the background electron density, and the value of EN is closely related with the characteristics of precipitating electrons (energy and flux). sz and sx correspond to the effective vertical and horizontal sizes of the perturbations, respectively.

4. Numerical Results

In the following computations, we have assumed the incidence of the 1st order mode. We calculate the wave fields scattered by the perturbation and the wave fields in the absence of the perturbation using the finite element method in a considered region. Because the purpose of this paper is to propose the use of FEM in estimating VLF wave fields in the presence of localized perturbations, we present a few figures to show the effectiveness of this FEM. Fig.3 illustrates the spatial distribution of the scattered field for a particular perturbation and at the frequency of 20kHz. The scattered field is defined as the difference between the perturbed and unperturbed fields. The perturbation is assumed to be located at x_0=100km and z_0=70km and other parameters are EN=100, sz=10km, and sx=25km. The top panel of Fig.3 is the computed 3-D plot of the amplitude of the scattered field $\mid H_y \mid$, and the bottom panel is the corresponding contour plot of the top panel seen from above. Fig.3 provides us with the mechanism of wave scattering from the perturbation. The dash-dot lines in the figure are calculated in the following way. The dash-dot lines are the trajectories of the constant phase difference between the direct wave from an effective point (in the perturbation)(x=25km and z=90km)and the wave reflected from the ground. The bottom dash-dot line corresponds to this phase difference of 0, the next upper one, 2π and so on. We can notice that the peaks of the scattered field follow approximately these dash-dot lines, and this figure will be useful to study the scattering mechanism.

Fig.4 shows the calculated change in amplitude, ΔA (a) and change in phase, $\Delta\phi$ (b) respectively, as would be observed at the receiver as a function of the GC path distance at frequencies of 5, 10, 16, and 20kHz. First of all, we find some oscillations in ΔA and $\Delta\phi$ in the distance left to the location of the perturbation, which are apparent to be due to the wave interference by the wave reflected from the perturbation. This point is a fundamental difference from the paper by Tolstoy et al. (1986). For f=5kHz, the changes in amplitude and phase, ΔA and $\Delta\phi$ respectively, become almost constant at a distance of about 600km(10λ) where a single dominant mode is propagated, with an advance in phase (positive $\Delta\phi$) and a reduction in amplitude (negative ΔA). Our numerical values of negative ΔA and positive $\Delta\phi$ are in agreement with the results deduced from the Earth-ionosphere waveguide mode theory that a reduction in height of the nighttime ionosphere gives rise to an increase in phase velocity and an increase in attenuation rate. It appears from the figure that the values of changes in amplitude and phase vary sinusoidally in the range from 0 to 600km at a frequency of 5kHz and in the range of 750 $\sim$ 1000km at the frequencies of 10, 16, and 20kHz. In these regions, two or more modes are required to represent the signal variations, and the ionospheric perturbations can produce significant mode conversions which means that single mode propagation is obviously violated.For higher frequencies of 10, 16 and 20 kHz, we do not have any stationary values in ΔA and $\Delta\phi$ in the distance range up to 1,500km. This may imply that a few modes are propagating in the waveguide. However, our numerical results indicate negative ΔA and positive $\Delta\phi$, on the average, on the GC paths beyond several hundred kilometers away from the center of perturbations, in agreement with the expected results deduced from the waveguide mode theory.

In this paper we will present many figures illustrating the frequency dependence, effects of enhancement factor, horizontal and vertical scale, and altitude of the perturbation etc..

5. Conclusion

In this paper we have proposed the use of the FEM in the analysis of VLF subionospheric propagation in the presence of localized perturbations in the lower ionosphere, and this FEM is found to provide us with the exact solutions. The 1st order mode is assumed to be incident into the waveguide, and we have found significant oscillations in the changes of amplitude and phase in the vicinity of the perturbation (distance less than 600 km), which is due to mode conversion and subsequent multiple mode propagation. The

detailed computational results will be compared with our corresponding observational results obtained in Australia and New Zealand in order to investigate the characteristics of the lightning- induced ionospheric perturbations.

References

Baba, K., and M. Hayakawa, Finite element method calculation of VLF propagation characteristics in the Earth-ionosphere waveguide. Trans.Inst.Elect.Inform.Comm.Engrs., Japan, J76-B-II, 244(1993).

Dowden, R.L. and C.D.D. Adams. Phase and amplitude perturbations on subionospheric signals explained in terms of echoes from lightning-induced electron precipitation ionization patches, J. Geophys. Res., 93. 11543(1988).

Helliwell, R.A., J.P. Katsufrakis, and M.L. Trimpi, Whistler-induced amplitude perturbation in VLF propagation, J. Geophys. Res., 78. 4679(1973).

Inan. U.S., and D.L.Carpenter, Lightning-induced electron precipitation events observed at L~2.4 as phase and amplitude perturbations on subionospheric VLF signals, J. Geophys. Res., 92,3293(1987).

McDonald, B.H. and A.Wexler. Finite-element solutions of unbounded field problems, IEEE Trans. MTT-20. 841 (1972).

Pappert, R.A. and F.P.Snyder. Some results of a mode-conversion program for VLF, Radio Sci., 7. 913 (1972).

Poulsen. W.L..T.F.Bell,and U.S.Inan, Three-dimensional modeling of subionospheric VLF propagation in the presence of localized D region perturbations associated with lightning, J.Geophys.Res., 95, 2355(1990).

Reagan, J.B., R.E. Meyerott, R.C.Gunton, W.L.Imhof, E.E.Gaines, and T.R.Larsen, Modeling of the ambient and disturbed ionospheric media pertinent to ELF/VLF propagation, AGARD Conference Proc. no.305(1982).

Rycroft.M.J., Interaction between whistler-mode waves and energetic electrons in the coupled system formed by the magnetosphere, ionosphere and atmosphere, J. Atmos. Terr. Phys., 53, 849(1991).

Tolstoy, A., T.J. Rosenberg. U.S.Inan, and D.L.Carpenter. Model prediction of subionospheric VLF signal perturbations resulting from localized electron precipitation-induced ionization enhancement regions, J.Geophys. Res., 91, 13473 (1986).

Wait, J.R., On phase changes in very-low-frequency propagation induced by an ionospheric depression of finite extent, J. Geophys. Res., 69, 441(1964).

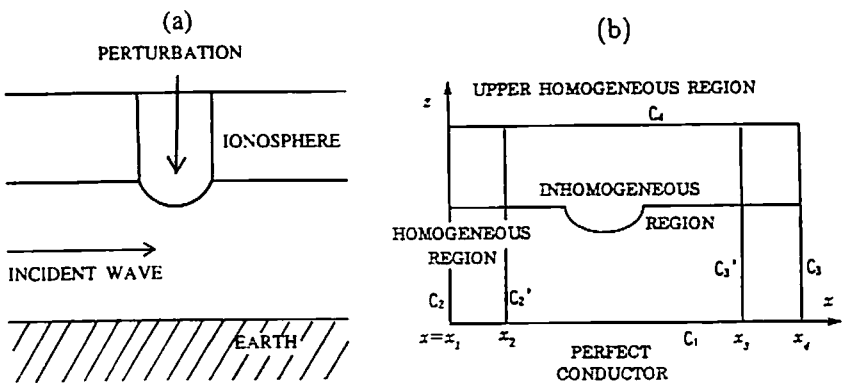

Fig.1 (a)Geometry of the Earth-ionosphere waveguide and (b)analysis space by means of finite element method.

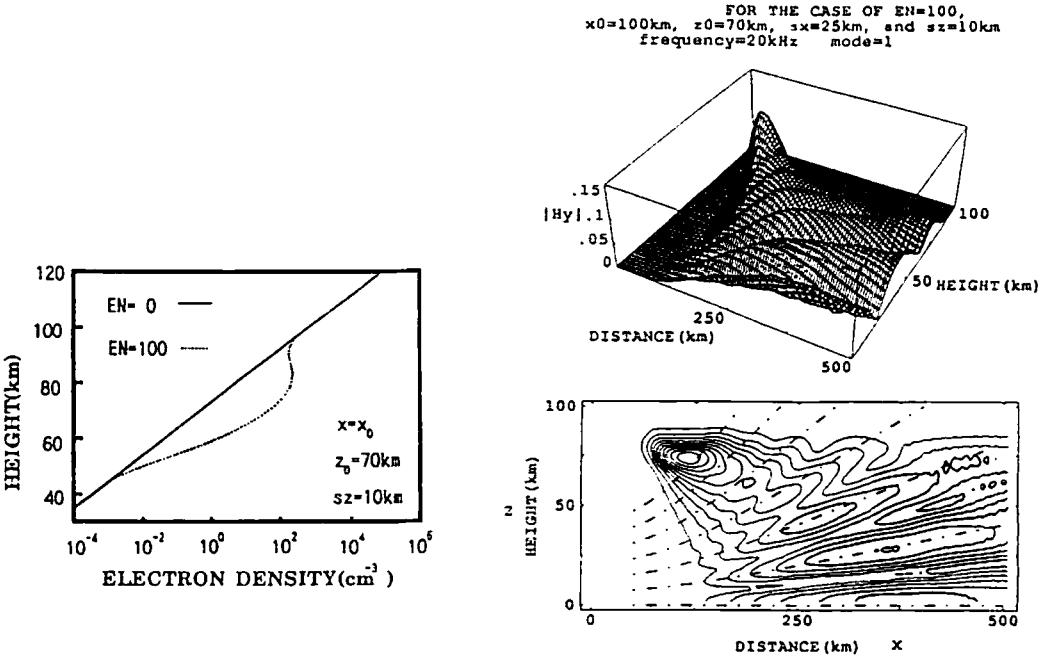

Fig.2 Electron density profiles. A full line represents the exponential profile without any perturbation, and a dotted line, an example of the localized perturbation (z_0 =70km) with EN = 100.

Fig.3 Spatial distribution of the scattered field (as the difference between the perturbed and unperturbed fields) for a particuler perturbation(x_0 = 100km, z_0 = 70km, sx = 25km, sz = 10km, and EN =100) at the frequency of 20 kHz. The top panel is the computed 3-D plot of the scattered field, and the bottom, the corresponding contour plot of the scattered field seen from above.

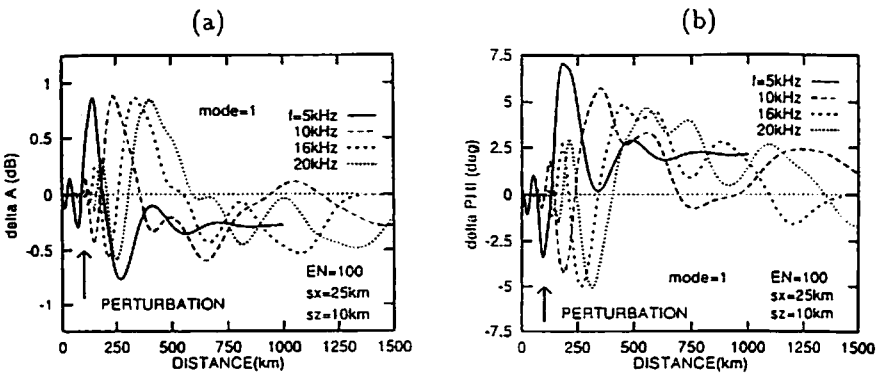

Fig.4 Variation of ΔA (a) and $\Delta\phi$ (b) due to the presence of the perturbation in Fig.3 as a function of distance. ΔA indicates the difference between the wave field with taking into account the perturbation and that without the perturbation, and $\Delta\phi$, the corresponding phase difference. An upward arrow indicates the position of the perturbation. Frequencies are 5,10.16 and 20 kHz.